Vibration monitoring of hydropower generator unit transformers for the purpose of winding set condition monitoring

B. Obaid
Electrical & Electronic
Engineering department
University of Canterbury
Private Bag 4800
Christchurch, New Zealand

W. G. Enright
Electrical & Electronic
Engineering department
University of Canterbury
Private Bag 4800
Christchurch, New Zealand

P. S. Bodger
Electrical & Electronic
Engineering department
University of Canterbury
Private Bag 4800
Christchurch, New Zealand

Introduction

Modern electrical machine maintenance practices are critically dependent on accurate condition monitoring techniques. The condition of power transformers is often assessed via traditional oil and electric tests. Unfortunately such tests are presently unable to determine transformer winding set clamping pressures. As critical clamping pressures relax with age, the likelihood of transformer failure due to short-circuiting increases. One proposed method for measuring the winding set condition is via tank wall vibration monitoring.

It must be emphasised that transformer tank wall vibration monitoring is presently a research topic. While some conference papers are available for review [1] [2] [3], there are no accepted International Standards or industry guidelines available for reference in this endeavour. It is interesting to note that researchers have attempted internal direct transformer vibration monitoring techniques [4]. This work gives crucial information regarding the vibration frequencies directly related to winding set conductor movement. Unfortunately the experiences associated with internal monitoring highlight poor instrumentation reliability. Furthermore one of the transformers under study failed due to an arc associated with the vibration sensors themselves.

This paper is divided into two main sections, the first section is the first principles derivation of two-conductor vibration, and the second section is conductor vibration from an energy perspective. The main aim of analysing the theoretical conductor vibration is to find an ideal footprint for the vibration patterns (this can be achieved by solving the associated governing equations). Then, this can be compared with the real spectrum of the vibration patterns. If the comparison error is not tolerable, then reasons may be attributed to the wrong positioning of the vibration pick-up device (accelerometer). The position of this can be changed in accordance with the calculated error.

The second section of this paper represents a new methodology for determining the tightness degree of the transformer winding clamping based on the energy content of the associated spectrum. Some practical examples based on the new methodology are given in the results section of this paper.

1. First Principles Derivation of Two-Conductor Vibration

The free-body diagram of one conductor is shown in Fig. 1. This shows the forces exerted on each conductor. Each conductor experiences a magnetic force F given by Equation (2.1)

$$F = \frac{\mu_o}{2\pi} \cdot \frac{i^2(t)}{d(t)} \quad \text{..... Equation (2.1)}$$

where

F = force per unit length
μ_o = permeability constant = 1.26×10^{-6} T.m/A
$i(t)$ = current in conductors a and b

$d(t)$ = displacement between the two conductors (distance of separation)

Also each conductor experiences other forces and undergoes some reactionary and stress forces. These forces are as follows: F_d is the deflection force resulting from the stress forces on each conductor. R is the reactionary force. Finally, F_g is the gravitational force, and this is given by $m.g$, where m is the mass of the conductor element and g is the acceleration due to gravity.

In Fig. 1, the acceleration $a(t)$ can be found by using the following equation:

$$F_t = ma = F - R + F_d + F_g \quad \text{..... Equation (2.2)}$$

where

F_t = total force on the conductor
m = mass of the conductor element

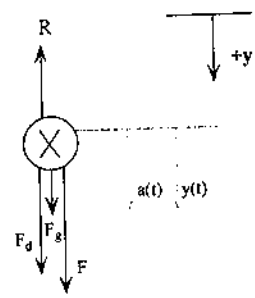

Fig. 1. A free-body diagram of one conductor carrying current i(t).

The acceleration in Equation (2.2) only depends on the magnetic force F and the reactionary force R. Under normal operation conditions, F_d and F_g are not taken into account because they contribute minimally when compared to F or R. From this argument, and given that m is a unit mass, and using Equation (2.1), an expression for $a(t)$ is obtained

$$a(t) = \left(\frac{\mu_o}{2\pi} \cdot \frac{i^2(t)}{d(t)} \right) - R \quad \text{.....Equation (2.3)}$$

Equation (2.3) can be further modified to include the second and first derivatives of $y(t)$, where the velocity $v(t)=y'(t)$ and the acceleration $a(t)=y''(t)$.

The displacement vector $y(t)$ can be written in terms of the separation displacement $d(t)$. This is achieved by the following steps (refer to Fig. 2(a) and Fig. 2(b)). A few assumptions are to be made or recalled before proceeding with the derivation steps: the conductors in Fig. 2(a) are exaggerated. They are assumed to be of negligible cross sectional area, of infinite length, and at the same time varying current flows into the page in both conductors. The two conductors are placed distance d apart at time zero. Another assumption is that conductor b can be treated as a mirror image of conductor a, i.e. conductor b has the same displacement, velocity, and acceleration as that for conductor a (with the opposite sign). Last but not least, the assumption is that the convention of Fig. 1 is followed.

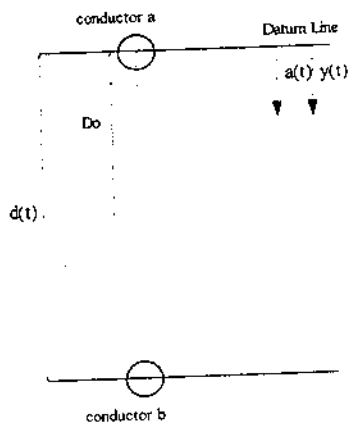

Fig. 2(a) Two conductors placed distance d apart at time zero. The two conductors are moving towards each other with a displacement of y(t) and an acceleration of a(t).

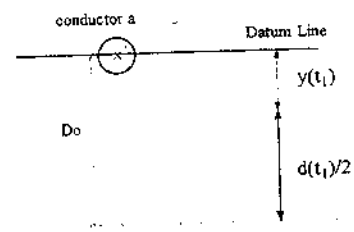

Fig. 2(b) The displacement of one conductor at $t = t1$.

The first step of deriving an equation for $y(t)$ in terms of $d(t)$ is to assign a datum line; let this be at the initial position (at time zero) of conductor a. The next step is to define a constant for the maximum

separation distance between one conductor and the center line; let this be D_o. By referring to Fig. 2(b), at time t_1, the conductor displacement $y(t_1)$ can be found by the following equation:

$$y(t_1) = D_o - \frac{d(t_1)}{2}$$

At any time, the displacement $y(t)$ is found, and this can be written in terms of the separation displacement $d(t)$; this is given by

$$d(t) = 2D_o - 2y(t) \quad \text{.....Equation (2.4)}$$

Equation (2.4) can be substituted in equation (2.3) to give

$$y''(t) = \left(\frac{\mu_o}{2\pi} \cdot \frac{i^2(t)}{2D_o - 2y(t)}\right) - R \quad \text{.....Equation (2.5)}$$

The reactionary force R in Equation (2.5) can be modelled as a spring-damper system. Each spring has a spring constant K, and each damper has a damping constant of B; the dampers account for the mechanical loses of the system (refer to Fig. 3). Given $y(t)$, K, and B, a general expression for R can be found.

Referring to Fig. 3, and noting that conductor b can be treated as a mirror image of conductor a, the following hold (considering conductor a): F_b is equal to $-F_a$, which is the magnetic force; y_b is equal to $-y_a$, which is the displacement function. Substituting the latter in $K(y_a-y_b)$ & $B(y'_a-y'_b)$ and writing the reactionary force in terms of the displacement y_a only, R_a is found to be (the subscript a was dropped)

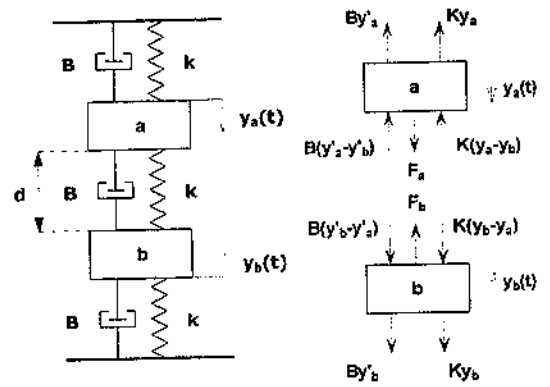

Fig. 3. The left hand side diagram represents the two-conductor system (mass-spring-damper system). The right hand side diagram represents the free body diagram of each conductor.

$$R = 3Ky(t) + 3By'(t) \quad \text{.....Equation (2.6)}$$

The above equation gives the magnitude of R, which can be substituted in Equation (2.5) (when Equation (2.5) was derived, the direction and sign of R were taken into account, so only the magnitude is required here). This gives the following equation:

$$y''(t) = \left(\frac{\mu_o}{2\pi} \cdot \frac{i^2(t)}{2D_o - 2y(t)}\right) - (3Ky(t) + 3By'(t)) \quad \text{.....Equation (2.7)}$$

Equation (2.7) is a second order non-linear differential equation. This equation cannot be solved analytically by simply applying the differential equation solving techniques. By solving this equation and transforming it into the frequency domain, the spectrum of the ideal conductor vibration of two conductors can be obtained. A mathematician is required to assist in solving this equation.

It can be seen that analysing the two-conductor system gave some complicated equations to be solved. This system represents the building block for analysing the more sophisticated system; the array of conductors in a practical power transformer helical low-voltage (l.v.) winding. It is anticipated that the equations for this system are even more complicated, because of the inherited non-linearity properties that prevents from applying the superposition principle. After arriving at this result, an empirical study should be considered.

2. Conductor Vibration From An Energy Perspective

2.1 Theory Behind The Associated Vibration Energy

As the winding sets loosen, the energy associated with transformer vibration will increase. The vibration energy $E(f)$ associated with any particular frequency f of vibration can be generally expressed as

$$E(f) = \frac{1}{2} m_e V^2(f) \quad \text{.....Equation (3.1)}$$

Where

m_e = the effective mass under vibration at sample point
$V(f)$ = the velocity amplitude at a particular frequency

Equation (3.1) is written in terms of the vibration velocity; a vibration energy equation in terms of the acceleration is required (the accelerometers attached to the exterior of the power transformers produce acceleration spectra). To obtain this, the acceleration was integrated in the time domain to obtain the velocity. This is given by the following equation:

$$v(t) = \int a(t)dt \quad \text{.....Equation (3.2)}$$

The above equation is written in the time domain; this can be transformed to the frequency domain using one of the Fourier transform properties [5]:

$$V(f) = \frac{A(f)}{j2\pi f} \quad \text{.....Equation (3.3)}$$

The acceleration $A(f)$ and the velocity $V(f)$ may consist of an imaginary part and a real part. These two parts are used to calculate the magnitude and the phase angle of $A(f)$ and $V(f)$; refer to the following equation:

$$|V(f)|\angle\theta(f) = \frac{|A(f)|\angle\phi(f)}{2\pi f\angle 90^\circ} \quad \text{.....Equation (3.4)}$$

where

$|V(f)|$ = magnitude of the velocity
$|A(f)|$ = magnitude of the acceleration
$\theta(f)$ = the velocity phase angle
$\phi(f)$ = the acceleration phase angle

For the purpose of this paper, only the magnitude is required. The velocity magnitude can be obtained from Equation (3.4) by

$$|V(f)| = \frac{|A(f)|}{2\pi f} \quad \text{.....Equation (3.5)}$$

After an expression for the acceleration amplitudes (magnitude of the acceleration at a particular frequency) was obtained, Equation (3.1) can be written in terms of the acceleration.

$$E(f) = \frac{1}{2} m_e \left(\frac{|A(f)|}{2\pi f} \right)^2 \quad \text{.....Equation (3.6)}$$

Equation (3.6) can be further modified to be

$$\frac{E(f)}{m_e} = \frac{1}{2}\left(\frac{|A(f)|}{2\pi f}\right)^2 \quad \text{.....Equation (3.7)}$$

Equation (3.7) represents the vibration energy associated with a particular frequency per effective mass. In theory, if the energy of the amplitudes is summed up at the frequencies that are multiple of the characteristic frequency, the energy content of an acceleration spectrum in a transformer that has tight winding sets is less than that in a one which has loose sets. This method is based on Parseval's theorem [6], where for a one-sided amplitude frequency spectra, Equation (3.7) holds. To check the validity of the hypothesis, the method was applied to practical results.

2.2 Results

The data presented in this section was obtained from transformers owned by Mighty River Power, which are located on the Waikato and Rotokawa Rivers of New Zealand. The readings were obtained from the Krippner conference paper [3].

The results were obtained for each transformer twice; the first test was performed prior to clamping the transformer winding sets, and the second was performed after the clamping stage was completed. Transformers that were refurbished (de-tanked, dry-out and re-clamped the windings) are referred to as **'new'**, and those prior to that stage are referred to as **'old'** transformers.

In this subsection, Equation (3.7) was used to calculate the sum of the energy content (refer to Table 1).

Transformer type Accelerometer Placement	Clamping status	Loading MW@MVAR	Sum of the energy content	Percentage difference
T7Y Front under side	Old	32@0	1.35e-7	**55% decrease**
T7R Front under side	New	32@0	6.0e-8	
T7Y Front upper midwall	Old	16@0	2.2e-7	**55% increase**
T7R Right hand midwall	New	16@0	4.9e-7	
***10R** Front lower midwall	Old	36@0	9.99-7	**97% decrease**
***6B** Front lower midwall	New	36@0	2.9e-8	
This portion of the table represents a comparison between the same transformers at different loadings				
T7Y Right hand midwall	Old	16@0	2.19e-7	**32% decrease**
T7Y Right hand midwall	Old	16@-14	1.49e-7	
T7R Front upper midwall	New	32@0	6.5e-7	**25% decrease**
T7R Front upper midwall	New	16@0	4.9e-7	

*They are of the same make and model (Ferranti single phase transformer 13333 kVA 11 to 220 kV G10 Red phase – SN 159195, Manufactured 1969. Not refurbished. G6 Blue phase – SN 159197, Manufactured 1969. Refurbished April 2000)

Table 1. A summary of the analysed Mighty River Power Transformers data

The results obtained from summing the energy associated with the frequencies (that are multiples of the characteristic frequency (using equation 3.7)), proved that as the winding sets loosen, the associated

energy increases. This result was not shown to be correct when comparing T7Y with T7R (16 MW 0MVAR) This is due to the fact that the location of the vibration monitoring devices is different in each case, where for T7Y the placement was on the right hand mid-wall of the transformer and on the other transformer (T7R) the device was placed on the front upper mid-wall.

Also, it can be noted that as the loading increases, the associated sum of energies and the sum of the acceleration amplitudes is always higher in the case of the higher loading rate, for the same transformer. This proves that it is inappropriate to compare transformers spectrum results under different loadings.

3. Conclusions

In conclusion, new techniques in vibration monitoring of power transformers were presented in this paper. The first technique's aim was to obtain an ideal footprint of the transformer conductor vibration to determine the optimal placement of the vibration monitoring devices on the exterior of the power transformer. This study failed, because of the complexity of the equations obtained from the 'simple' two-conductor system (an array of the conductor system is required for the complete analysis).

The second technique presents a new approach for analysing acceleration spectra obtained from the accelerometers mounted on the exterior of the power transformer. This was based on calculating the associated energy of the acceleration spectra. Results obtained from transformers owned by Mighty River Power were analysed; the expected results agreed with those obtained from the real results analysis. Also, it was shown that it is only appropriate to compare results obtained from transformers that are of the same type and make, and when the same conditions were applied during the tests – for example, the transformer loading and oil temperature.

References

1. **Mechefske, C. K.,** "Assessing the internal mechanical integrity of power transformers using tank wall vibrations", *CM2 Forum* 1996.

2. **Marques Cardoso, A. J. and Oliveira, L. M. R.,** "Condition monitoring and diagnostics of power transformers", *Proceedings*, COMADEM 1998.

3. **Krippner, D.,** "Development Of A Power Transformer Condition Monitoring Program Through Vibration Analysis". *Conference*, VANS (Vibration Association of NZ Inc) 2001.

4. **SanzBobi, M. A., GarciaCerrada, A., Palacios, R. and Villar, J.,** "Experiences learned from the on-line internal monitoring and the behaviour of a transformer", *IEEE International Electric Machines and Drives Conference*, Milwaukee, 1997.

5. **Haykin, S. S.,** "Communication Systems", 3rd ed, New York , Wiley, 1994. Pp 42

6. **Stuller C.,** "Circuit Analysis", 2nd Ed., USA, 1995. Pp550-552.

The Authors

B. Obaid: is studying towards the completion of a BE (Hons) degree in electrical and electronic engineering at the University of Canterbury. During 1999 she worked for the Computer Science department at the University of Canterbury as a full-time research assistant/programmer - research topic: Adaptive Video Indexing Methods.

W. G. Enright: completed his BE (Hons) and PhD degrees in electrical and electronic engineering from the University of Canterbury in 1992 and 1995 respectively. During 1996 he worked for the Manitoba HVdc Research Centre in Winnipeg, Canada. He spent 1997 with the Electricity Corporation of New Zealand Ltd. In 1998 he returned to the University of Canterbury to continue Power Systems Research. In 1999 Wade formed is own professional engineering company "Viva." Through "Viva" he now offers technical services to industry and lectures at the University of Canterbury as a consultant.

P. S. Bodger: completed his BE (Hons), PhD and P.Eng degrees in electrical and electronic engineering from the University of Canterbury. He worked as an assistant engineer, NZ Electricity (Design and Construction, Power Station Maintenance) in 1977-80. He worked as an engineer for NZ Electricity (Commercial section) in 1981. He has commercial experience as a Shareholder and Director of new technology companies: Transflux Holdings Ltd, Ennotech Holdings Ltd, and Watcon Developments Ltd. He represents: the NZ Delegate, Commission K: Electromagnetics in Medicine and Biology, URSI and the Board of Directors, Centre for Advanced Engineering.